Dalton Transactions

ROYAL SOCIETY OF CHEMISTRY

PAPER

View Article Online
View Journal | View Issue

Cite this: *Dalton Trans.*, 2020, **49**, 14975

Synthesis and characterization of the mixed-ligand coordination polymer $Cu_3Cl(N_4C\text{-}NO_2)_2$†

Bradley Westwater,[a] Hayleigh J. Lloyd,[b] Inigo J. Vitorica-Yrezabal,[c] Angela Fong,[b] Patrick McMaster,[d] Martin Sloan,[d] Brian M. Coaker,[e] Colin R. Pulham[b] and Peter Portius*[a]

Received 2nd September 2020,
Accepted 13th October 2020

DOI: 10.1039/d0dt03077e

rsc.li/dalton

Reduction of copper(II) chloride using sodium ascorbate in the presence of pure sodium 5-nitro-tetrazolate (NaNT) forms copper(I) 5-nitrotetrazolate – a known initiatory explosive (DBX-1) – and the novel mixed-ligand copper(I) chloride 5-nitrotetrazolate coordination polymer $Cu_3Cl(N_4C\text{-}NO_2)_2$, as well as mixtures of both. The reaction is controlled by the presence of seed crystals and transition metal compounds other than $CuCl_2$. $Cu_3Cl(N_4C\text{-}NO_2)_2$ is obtained as a wine-red, air stable, water-insoluble, crystalline and highly sensitive explosive material with a greater crystal density, lower thermal stability and a higher sensitivity toward hydrolysis and shock than DBX-1. Efforts to obtain the stable and pure starting material are improved by crystallisation of NaNT as a tetrahydrate. $Cu_3Cl(N_4C\text{-}NO_2)_2$ and $Na(H_2O)_4(NT)$ were characterised by single crystal and powder XRD, IR spectroscopy, magnetic and thermal measaurements, elemental analysis, particle size measurements, mass spectrometry, and by drop weight testing.

1. Introduction

Lead-free energetic compounds with high thermal and hydrolytic stability are highly sought-after materials in current efforts to replace lead-containing initiatory explosives such as lead azide and lead styphnate.[1–5] Although well-characterised and effective in their intended use, the latter compounds should be replaced due to the deleterious effects of their heavy metal content, which is present in all stages of their manufacture, storage, processing, use, remediation, and disposal. A number of alternatives with fewer health and environmental issues have been investigated and include, amongst others, 5-nitro-(1*H*)-tetrazolates of silver[6,7,14,18] and, in particular, copper azides and nitrotetrazolates (DBX-1).[8–12] DBX-1 is a member of a family of energetic copper nitrotetrazolates consisting of $Cu(en)_2(NT)_2$,[14] $Cu(NH_3)_3(NT)_2$,[14] $(M')_2[Cu^{2+}(NT)_4{\cdot}(H_2O)_2]$,[15] copper(I) nitrotetrazolate[16,17] or DBX-1,[8,9] $Cu(NT)_2$ [18] and $Cu(H_3O)(NT)_3{\cdot}3H_2O$[10,13,19] (en = ethylene diamine, NT = 5-nitrotetrazolate). The synthesis of DBX-1 is not straightforward. There is a lack of insight into the mechanism of its formation in the presence of sodium 5-nitrotetrazolate (NaNT) by reduction of either copper(II) chloride with sodium ascorbate, Na(HAsc), in an aqueous reaction mixture (Scheme 1),[16,17,20] or from copper(I) chloride directly.[17,21] Efforts to achieve repeatable, consistent and efficient synthesis of DBX-1 have driven research into testing specific preparative methods.[8–10] The quality of the starting material NaNT as the nitrotetrazolyl group transfer reagent[14] is critical. This area was explored by Klapötke[9] and lead to a purification method involving aqueous NaNT solutions and ion-exchange resin (see ref. 22 and 23 for further modifications). Ford and co-workers have reported a one-pot method as part of a lean process for the production of DBX-1 which requires neither the isolation of NaNT, nor its purification.[10] Omitting purification by this new method reduces the extent of the protective measures needed to keep operational hazards at acceptably low levels and it therefore improves the safety of the syn-

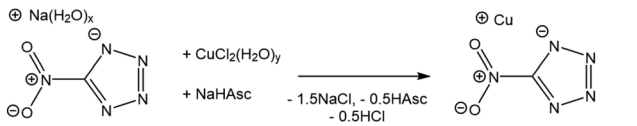

Scheme 1 Reaction of NaNT hydrate, copper(II) chloride and sodium ascorbate, Na(HAsc), in an aqueous reaction medium to form copper(I) 5-nitrotetrazolate (DBX-1).

[a]*Department of Chemistry, University of Sheffield, SheffieldWestern Bank, S3 7HF, UK. E-mail: p.portius@sheffield.ac.uk*
[b]*School of Chemistry, University of Edinburgh, Edinburgh, EH9 3FJ, UK*
[c]*School of Chemistry, University of Manchester, ManchesterOxford Rd., M13 9PL, UK*
[d]*Ministry of Defence, Abbey Wood, Bristol, BS34 8JH, UK*
[e]*Managing Consultant, Munitor Engineering Services Limited, Leasingham, Lincolnshire, NG34 8LJ, UK*

†Electronic supplementary information (ESI) available: Microscope images, diffractograms, IR, UV/vis and spectra, calorigrams, preparative conditions. CCDC 1968822 (2) and 1983373 (3). For ESI and crystallographic data in CIF or other electronic format see DOI: 10.1039/d0dt03077e

thesis. Fronabarger and colleagues found that the nitric acid needed for the synthesis of NaNT can be replaced by the more cost effective sulphuric acid.[22] It was noted that the mechanism of the DBX-1 formation is composed of several steps and begins with an induction period in which $Cu(H_3O)(NT)_3{\cdot}3H_2O$ (*vide supra*) acts as an intermediate. Ford and co-workers suggested that crystal seeds play a role.[10] Finally, Fronabarger provided a detailed preparative method for the synthesis of DBX-1 and reported yields ranging from 80% to 85%.[8,9,24,25] Neither polymorphs of DBX-1, nor any by-products other than the aforementioned $Cu(H_3O)(NT)_3{\cdot}3H_2O$, are known.

In this paper, we detail results of an in-depth investigation into the selectivity of the reduction reaction discussed above, which forms not just DBX-1, but also a previously unreported compound depending on reaction conditions. Physicochemical properties of the new copper-containing properties are determined. The nitrotetrazolate starting material is investigated further regarding its structure and suitability for the reduction reaction.

2. Experimental section

2.1. Materials and instrumentation

Caution (!), compounds **3** and **4** are highly sensitive to heat, friction, and impact and will explode if stimulated. Appropriate protective equipment and safe preparative methods should always be used when working with these materials. Copper(II) chloride (Lancaster, anhydrous, 98%) was used either as purchased, or after recrystallization from deionized water as $CuCl_2(H_2O)_2$. Both compounds were stored in airtight containers prior to use. Sodium 5-nitrotetrazolate (NaNT) was prepared according to a published procedure,[9] which involves the slow evaporation of an acetone extraction solution at r.t. to afford the dihydrate $NaNT{\cdot}2H_2O$ (**1**). Preliminary and qualitative data on impact and friction sensitivities were obtained using the drop-weight tester at Sheffield, and an agate mortar and pestle, respectively. Impact sensitivity data is given as the interpolated energy (E_{50}) at which initiation occurs with a 50% probability (NB: using the same apparatus and method, E_{50} of synthesis-grade RDX was found to be 5.3 (±0.2) J). Thermograms were recorded in the temperature range 50 to 350 °C and at the stated heating rates, using a TA Instruments DSC 25 Discovery Series calorimeter and sealed Perkin Elmer stainless steel sample containers (30 μL internal volume, Au-plated Cu seals, T_{max} = 400 °C, p_{max} = 150 bar). The calorimeter was calibrated against In (99.999%) at the 156.60 °C transition (ΔH = 28.45 J g^{-1}). IR spectra were obtained from mulled (liquid paraffin) samples between NaCl windows using a Bruker Vector FTIR spectrometer at an optical resolution of 2 cm^{-1} in the spectral range 4000 to 500 cm^{-1} over 8 scans. Susceptibility measurements were carried out at 25 °C with a magnetic susceptibility balance (Sherwood Scientific, Cambridge, UK). Copper content was determined spectrophotometrically in aqueous medium at 803 nm using the spectral properties of $Cu(H_2O)_6^{2+}$ published by Qiu *et al.*[26] and extrapolated to 20 °C; the stated Cu content is derived from four samples. Mass spectral data was obtained using the MALDI TOF method and a DCTB (*trans*-2-[3-(4-^{t}Bu-phenyl)-2-methyl-2-propenylidene]malononitrile) matrix made from a slurry of **3** in CH_2Cl_2–DCTB solution. The particle morphology was characterized both microscopically and with a Malvern Particle Size Analyser "Master Sizer 3000" in water applying the Fraunhofer diffraction pattern analysis. Single crystal X-ray data for compound **3** were collected at a Rigaku FR-X diffractometer equipped with an ultra-high-intensity microfocus rotating anode X-ray generator, a HypixHE6000 detector, an Oxford Cryosystems N_2 gas flow cooling system, and Cu-K_α radiation. Data were recorded, processed and reduced using the CrysAlisPro suite of programs. Absorption correction was performed with empirical methods (SCALE3 ABSPACK) based on symmetry-equivalent reflections combined with measurements at different azimuthal angles.[27–29] SIMU and RIGU SHELX restrains were used to model the atomic displacement parameters. Intensity data for $NaNT{\cdot}4H_2O$ (**2**) were collected on a Bruker D8 Venture diffractometer equipped with a Photon 100 CMOS detector using a Cu-K_α microfocus X-ray source from crystals mounted in fomblin oil on a MiTiGen microloop and cooled in a stream of cold N_2. Data were absorption-corrected with empirical methods (SADABS)[30] based on symmetry-equivalent reflections combined with measurements at different azimuthal angles.[28] Both crystal structures were solved and refined against all F^2 values using ShelXT, ShelXL and Olex 2 suites of programmes.[31,32] All non-H atoms were refined anisotropically after their positions had first been found in the Fourier map and then refined with the O–H bond lengths restrained. PXRD data for compound **3** was recorded at the University of Sheffield on a Bruker D8 ADVANCE powder X-ray diffractometer equipped with a Cu-K_α sealed-tube source, a focusing Göbel Mirror operating in capillary mode, and an Oxford Cryosystems Cryostream Plus 700 series low-temperature unit, allowing for variable temperature measurements. PXRD Samples were prepared by packing powder of **3** into 0.7 mm borosilicate sample capillaries. During data collection, capillaries were centred and rotated at 30 rpm. Data were collected at both 298 K and 113 K in the range $3° \leq 2\theta \leq 70°$ with the step size of 0.015° and step time of 1.8 s, giving a total exposure time of 2 h 15 min. Further crystallographic data can be found in the ESI.†

2.2 Synthesis of sodium nitrotetrazolate tetrahydrate, Na(NT)·4H$_2$O (2)

In a glass beaker, a saturated solution of sodium 5-nitrotetrazolate was prepared by stirring $Na(NT){\cdot}2H_2O$ (**1**), (173.02 g mol^{-1}, 7.905 g, 45.7 mmol, obtained by crystallisation at r.t.) in deionised water (*ca.* 18 ml) at 20 to 25 °C. By immersing the beaker in an ice bath, the solution was then cooled to 0 °C for the duration of 2 h, after which needle-shaped colourless crystals had formed. Cold-filtration, washing of the filter residue with small amounts of ice-cold water (×2) and then acetone (×2), followed by brief air-drying of the wash residue, affords

compound **2** ($CH_8N_5NaO_6$, 209.04 g mol^{-1}, 5.943 g, 28.4 mmol, 62% with respect to **1**) as a white crop of colourless, odourless, free-flowing crystals. Compound **2** can be stored in a sealed vessel without decomposition at r.t. for several months. Under a dynamic vacuum (*ca.* 1 mbar) at r.t., however, it dehydrates readily to convert into **1** (IR spectra in Fig. S7 to S9†). The yield afforded by this preparative method is highly sensitive to temperature and solvent volumes, and ranges between 29% and 62%. IR (nujol) ν/cm^{-1} = 3592s, 3399s, br, 1643w, 1551s, 1453vs, 1426vs, 1325s, 1183m, 1058w, 1035w, 842m, 597vs, br (Fig. S8†). Magnetic susceptibility χ_{meas}/(emu mol^{-1}) = −4.2 (±0.7) × 10^{-4}. A suitably sized specimen of the crop was used for the single crystal XRD study (*vide infra*).

2.3. Synthesis of chloro(nitrotetrazolato)copper(I) (3)

$CuCl_2(H_2O)_x$ (x = 0 or 2) was reduced using the method given by Fronabarger *et al.*[8] (*vide supra*) apart from the following modifications to apparatus and reagents (i–iv): a 100 ml beaker made from borosilicate glass acts as the reaction vessel (i), a Teflon-coated magnetic bar with the dimensions 25 mm × 6 mm is employed for agitation (ii), compound **2** is used as the nitrotetrazolyl group transfer reagent (iii), and the aqueous Na(HAsc) reductant is added dropwise into the reaction mixture using a Pasteur pipette (iv). NB: previous publications noted colour changes upon addition of the nitrotetrazolyl group transfer reagent. We have found that they are dependent on the purity of the NaNT solution; addition of **1** results in a colour change from light blue to green; however, the addition of aqueous solutions of **2** to those of $CuCl_2$ causes a slight deepening of the blue colour. The Na(HAsc) addition regime was (points in time stated in minutes, reaction mixture stirred continuously): 0 to 1.5 addition, 1.5 to 6 dwell time, 6 to 13.5 addition, 13.5 to 15 dwell time. Four experiments were executed under the stated conditions, which produced compound **3** exclusively. The isolated yields with respect to $CuCl_2$ range from 67% to 86% (see microscope images Fig. S21†). **Caution (!)**, careful grinding of a 10 mg batch of **3** obtained by this preparative procedure, using an agate mortar and pestle, caused initiation events (audible as loud crackling sound), which subsided once the crystal size had reduced sufficiently through milling action. $Cu_3Cl(N_4CNO_2)_2$ (**3**), M = 454.18 g mol^{-1}; DSC, T_{on} = 274 °C (dec.), T_{peak} = 283 °C, ΔH_{exo} = 1201 J g^{-1}, 3 K min^{-1}, NB: heating compound **3** at a high rate (10 K min^{-1}) causes decomposition at around 300 °C and breaks the sample container. Cu content as Cu^{2+} 41.97(±0.04)% (calcd), 41.7 (±2.4)% (found). In three crops of crystals, the magnetic susceptibility χ_{meas}/(emu mol^{-1}) was found to range from −8.4 (±0.5) × 10^{-4} to +1.8(±0.2) × 10^{-4}. IR (nujol) ν/cm^{-1} = 1563vs, 1550m, 1486w, 1430w, 1422w, 1328s, 1292vw, 1197vw, 1084vw, 1071vw, 1045vw, 838m, 833m, 768vw, 715w, 662w, 502vw; IR (KBr) ν/cm^{-1} = 1564vs, 1550s, 1486w, 1463s, 1458m, 1429m, 1421m, 1327s, 1084vw, 1071vw, 1045vw, 838m, 832m, 714vw, 662w; TOF LD(+) MS m/z = 652 (2) $[Cu_2(CN)(DCTB)_2]^+$, 563 (8) $[Cu(DCTB)_2]^+$, 502 (4) $[Cu_4(DCTB)]^+$, 418 (9) $[Cu_2O(CN)(DCTB)]^+$, 411 (11) $[Cu_2Cl(DCTB)]^+$, 402 (21) $[Cu_2(CN)(DCTB)]^+$, 313 (100) $[Cu(DCTB)]^+$, 241 (8) $[Cu_3(CN)_2]^+$, 152 (5) $[Cu_2(CN)]^+$. PXRD data (Fig. S5†) and single crystal data are given elsewhere and in the ESI.† A suitably sized, but small, specimen crystal was used for single crystal XRD measurement (*vide supra*). Impact sensitivity E_{50} = 1.8(±0.2) J. For comparative purposes, analogous analytical data for $Cu(N_4CNO_2)$ (**4** "DBX-1", M = 177.59 g mol^{-1}), obtained at Sheffield under identical conditions, are given here: DSC, T_{on} = 293 °C (dec.), T_{peak} = 305 °C, ΔH_{ex} = 1653 J g^{-1}, 3 K min^{-1}. IR (nujol) ν/cm^{-1} = 1558vs, 1548vs, 1489m, 1472s, 1454s, 1425s, 1327vs, 1201vw, 1189vw, 1164vw, 1123vw, 1098w, 1079vw, 1047vw, 1040vw, 835vs, 768vw, 718w, 671w, 655w, 552w; impact sensitivity E_{50} = 4.3(±0.3) J. PXRD data are given in Fig. S3.† Data available for DBX-1 in the cited literature: DSC: T_{on}/°C = 302.8 (5 K min^{-1}),[10] 329.8 (20 K min^{-1}),[8] T_{peak}/°C = 337.7 (20 K min^{-1}),[8] ΔH_{ex} = 1967 J g^{-1}, (20 K min^{-1}); IR (KBr) ν/cm^{-1} = 1556vs, 1470s, 1451m, 1422s, 1325vs, 1123w, 1096w, 832s; crystal structure see ref. 8, PXRD ref. 10.

3. Results and discussion

Depending on reaction conditions and starting materials in the reduction of aqueous solutions of copper chloride and sodium 5-nitrotetrazolate with sodium ascorbate, three types of precipitate were obtained. These are a powder of unknown composition, the previously reported $Cu(N_4C\text{-}NO_2)$ (**4**), and the novel $Cu_3Cl(N_4C\text{-}NO_2)_2$ (**3**). As the reduction reaction is highly sensitive to impurities in the starting material, the crystallisation conditions of NaNT for the purpose of purification are examined first.

3.1 Sodium 5-nitrotetrazolate tetrahydrate (2)

At a crystallization temperature of 0 °C, NaNT forms a novel hydrate (**2**) as transparent, completely colourless, needle-shaped crystals the IR spectrum of which is closely related to that of the previously reported NaNT·2H_2O (**1**). Under vacuum and at r.t., **2** readily converts into **1**, and then into water-free NaNT (see Fig. S7–10,† NB: **1** forms directly by evaporation of aqueous solutions at r.t.[9]). The dehydration process can be monitored easily in the infrared using the peak absorption cross sections at ν/cm^{-1} = 1191, 1178, 1068, 1057, 1040 (water-free NaNT), 1193, 1173, 1066 and 1041 (**1**), 1183, 1173, 1058, 1035 (**2**). In a sealed vessel at r.t. and ambient pressure, compound **2** is stable indefinitely. Using single crystal X-ray methods, the nature of the crystalline **2** was probed further with details given below (Table 1).

Crystals of **2** consist of hydrated NaNT and water of crystallisation, $Na(H_2O)_2(NT)\cdot 2H_2O$, in which sodium is coordinated in a distorted octahedral geometry (Fig. 1, top, showing $Na(OH_2)_4(\kappa O\text{-}NT)(\kappa N_\beta\text{-}NT)$) with bridging water and 5-nitrotetrazolato ligands. Cations are arranged in linear $\{Na(OH_2)_2\}_n$ chains through μ^2-aqua bridges (Fig. 1, middle). The chains are interconnected by $H_2O\cdots(H_2O)\cdots OH_2$ hydrogen bonds to form $[(H_2O)\cdots\{Na(OH_2)_2\}\cdots(H_2O)]_n$ sheets, which are directed into a collinear arrangement *via* $Na\cdots O_2N\text{-}CN_4\cdots Na$ links (Fig. 1, bottom). A comparison with the dihydrate **1** (Table 2; see ref.

Table 1 Crystal data and structure refinement parameters for $Na(N_4C\text{-}NO_2)\cdot 4H_2O$ (**2**) and $Cu_3Cl(N_4C\text{-}NO_2)_2$ (**3**)

	2	**3**
Empirical formula	$CH_8N_5NaO_6$	$C_2ClCu_3N_{10}O_4$
Formula weight	209.11 g mol^{-1}	454.19 g mol^{-1}
Temperature	100.0(3) K	100.0(3) K
Crystal system	Monoclinic	Monoclinic
Space group	$C2/c$	$P2_1/c$
Unit cell dimensions	a = 17.7189(10) Å, b = 3.5053(2) Å, c = 13.3457(8) Å, α = 90°, β = 100.282(2)°, γ = 90°	a = 10.8980(10) Å, b = 9.2377(9) Å, c = 10.3680(10) Å, α = 90°, β = 100.493(10)°, γ = 90°
Volume	815.59(8) Å^3	1026.32(17) Å^3
Z	4	4
Density (calculated)	1.703 Mg m^{-3}	2.939 Mg m^{-3}
Absorption coefficient	1.925 mm^{-1}	10.046 mm^{-1}
F(000)	432.0	872.0
Crystal size/mm^3	0.345 × 0.21 × 0.15	0.01 × 0.01 × 0.01
Radiation	CuK_α (λ = 1.54178)	CuK_α (λ = 1.54184)
2Θ range data collection	10.146° to 133.482°	8.252° to 152.288°
Index ranges	$-20 \le h \le 20$; $-3 \le k \le 4$; $-15 \le l \le 15$	$-10 \le h \le 13$; $-11 \le k \le 11$; $-11 \le l \le 12$
Reflections collected	9009	4254
Independent reflections	710 [R_{int} = 0.0661]	2060 [R_{int} = 0.1114]
Data/restraints/param.	710/64/109	2060/84/181
Goodness-of-fit on F^2	1.179	1.066
Final R indexes [$I \ge 2\sigma(I)$]	R_1 = 0.0389, wR_2 = 0.0991	R_1 = 0.0569, wR_2 = 0.1200
Final R indexes [all data]	R_1 = 0.0408, wR_2 = 0.1002	R_1 = 0.1046, wR_2 = 0.1429
Largest diff. peak/hole	0.30/−0.30 e Å^{-3}	1.01/−0.93 e Å^{-3}

33 and 34 for structure data of **1** and $NaNT\cdot H_2O\cdot 0.5MeCN$) reveals unique structure features of **2**: the NT ligands in **1** coordinate in bidentate fashion ($Na(OH_2)_2(\kappa^2N_\alpha,O\text{-}NT)(\kappa N_\beta\text{-}NT)$) whereas only monodentate modes are observed in **2**. This mode change results in much greater distortion from octahedral geometry for sodium in **1**. There are no bridging H_2O ligands in **1**, whereas in **2** all aqua ligands are part of Na···O···Na bridges. Even though in **1**, all water is coordinated to Na, and only half of the water is in **2**, only negligible differences in the Na–O distances of coordinated water are found (**1**, 2.37, 2.39 Å; **2** 2.38, 2.39 Å). In **1**, the Na–Na linkage is made by $\mu^3(O',N_\alpha,N_\beta)$-NT bridges (two per centre); however, bridging in **2** relies on $\mu^2(O)$-H_2O (four) and $\mu^2(O,N_\beta)$-NT (two) coordination resulting in a greater degree of interlinkage in the latter. It is worth noting that the Na···O_2N contacts in **1** are 0.1 Å longer than in **2**, whereas the Na···N_βNT bonds are 0.1 Å shorter. This contraction–elongation effect is ascribed to the chelating coordination mode of the μ^3-(O,N_α,N_β)-NT ligand in **1** as opposed to **2** in which NT acts as simple μ^2-(O,N_β)-NT linker only. Despite these variations, there are no significant changes to the intramolecular bond lengths and angles of the NT ligand. Since the Na···O_2N-CN_4 and Na···N_4C-NO_2 bonds are long and weak, it must be concluded that the variations in the coordination networks **1** *vs.* **2** have negligible effect on the enthalpic contributions of the NT group (*vide infra*) to the heat of decomposition of bot compounds. If hydration, hydrogen bonding and lattice enthalpies are not accounted for, and based on the enthalpic contribution of the NT content alone, then the energy density of **2** must be smaller in comparison to **1** (2.4 *vs.* 2.9 kJ cm^{-3}, *vide infra* and Table S2†) and this indicates that the tetrahydrate is an attractive alternative storable solid nitrotetrazolato group transfer reagent.

3.2 Reduction reactions using crystallized sodium 5-nitrotetrazolate hydrates

The tetrahydrate described above was employed in reduction reactions of $CuCl_2$ with Na(HAsc) and NaNT in adaptation to the previously published method for the synthesis of copper(I) 5-nitrotetrazolate (**4**, "DBX-1") (see Experimental section). Our experimental results confirm the adverse effect of impurities in the NaNT starting material in a similar fashion as they were noted before (see Introduction). The application of the crystallised $NaNT\cdot 2H_2O$ (**1**) as the nitrotetrazolyl reagent in adaptation to the previously published reaction regime over the course of 15 minutes, affords an orange, suspended material that readily blocks D4 sinter filter and discolours over time in air to form an olive-green, highly explosive powder of yet unknown composition. Repeating the reduction under otherwise identical conditions in the same reaction vessel, and replacing the dihydrate **1** by the crystallised tetrahydrate **2**, however, afforded a wine-red precipitate (compound **3**), and no DBX-1 was obtained. The visual appearance and IR spectrum of **3** are distinct from those of the orange to rust-red DBX-1 (**4**) (see photographs in Fig. 2, left (**3**) *vs.* right (**4**), and the IR spectra in Fig. 5 and S11–15†). The experiment was repeated another four times over the course of several weeks to give unaltered results at each instance. A number of factors were tested. Neither a replacement of Teflon-coated stir bars, of $CuCl_2$ for $CuCl_2\cdot 2H_2O$, and of deionized for distilled water, nor small changes in the addition time and addition regimen had a significant effect. The identity of the four batches of the new crystalline product with that obtained originally was established by comparison of IR spectral data and PXRD data (*vide infra*). The new material (**3**) consists of dark wine-red,

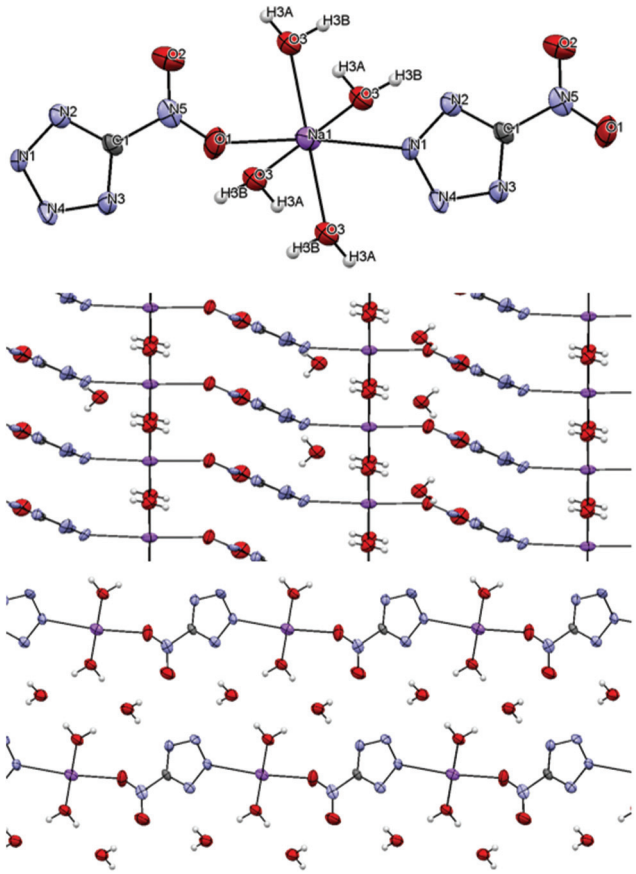

Fig. 1 Thermal ellipsoids projection (90% probability level) of the crystal structure of NaNT·4H_2O (2) (coordination of Na, top; Na ··· (H_2O) ··· Na link (middle); Na ··· O_2N-CN_4 ··· Na link (bottom, H_2O ··· H-OH bonds involving water of crystallization not shown); O, red; Na, purple; C; dark grey, H, light grey, N, blue. One disordered part of the O_2N-CN_4 moiety is shown; selected bond lengths: Na01–O2 2.359(15), Na01–O1W 2.378(3), Na01–O1W 2.394(3), Na01–N3 2.594(15), N1–N2 1.349 (14), N1–N3 1.350(14), N2–C1 1.330(4), N3–N4 1.331(15), N4–C1 1.334 (5), C1–N5 1.447(5), N5–O2 1.236(9), N5–O1 1.240(9).

glistening, friction- and impact-sensitive crystals. It is insoluble in CH_2Cl_2, cold DMF and iPrOH, but dissolves in DMSO and hot DMF under decomposition. As compound **4**, so

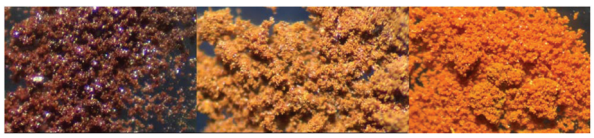

Fig. 2 Microscope images of pure compound **3** (left), of a **3**–**4** mixture (middle), and of pure **4** (right); all images taken at the same magnification.

does compound **3** dissolve completely in aqueous nitric acid (65%) to form a solution with a colour characteristic of Cu^{2+} (the UV/vis spectrum, Fig. S16,† features a broad peak at 803 nm characteristic for the aqua complex[26]). Its magnetic susceptibility was found to be approximately -6×10^{-7} emu g^{-1} which is comparable with that predicted using the increment method,[35] $\chi_{pred} \approx -5 \times 10^{-7}$ emu g^{-1} suggesting that the material is diamagnetic and contains Cu(I) exclusively. Apart from copper, no other metals could be detected using MALDI mass spectrometry (Fig. S22†), hence the presence of nickel or zinc as contaminants affecting the outcome of the reaction must be excluded.

3.3 Structure analysis of compound 3

Single crystal X-ray diffraction measurements were performed using selected crystals from one batch of **3** (see Fig. 2, S1, S21,† crystal data Table 1). The small crystal size required a high-flux rotating anode as X-ray source. Crystalline **3** is composed of copper, chlorine and 5-nitrotetrazolyl moieties which are distributed over three, one and two unique crystallographic sites in the stoichiometric ratio of 3 : 1 : 2, respectively. These proportions, in combination with the measured magnetic properties, imply that copper is exclusively present in the oxidation state +1 forming the compound $Cu_3Cl(N_4C\text{-}NO_2)_2$ (**3**). Copper is coordinated to at least one chloro- and up to three nitrotetrazolato ligands in variously distorted tetrahedral fashion, forming Cu(κ(N1)-NT)(κ(N2)-NT)Cl_2, Cu(κ(N1)-NT)(κ(N2)-NT)$_2$Cl and Cu(κ(N1)-NT)$_2$(κ(N2)-NT)Cl environments (Fig. 3 bottom) that constitute a mixed-ligand coordination polymer (Fig. 3, top).[36,37] Differently to **2** and **4**, all ring-nitrogen atoms are engaged in the coordination network involving

Table 2 Key bond lengths/Å[a] in the crystal structures of Na(N_4C-NO_2)·2H_2O (**1**),[c] Na(N_4C-NO_2)·4H_2O (**2**), $Cu_3Cl(N_4C\text{-}NO_2)_2$ (**3**) and Cu(N_4C-NO_2) (**4**)[d]

	1[c]	**2**	**3**	**4**[d]
M–N_α	2.466(1)	—	1.968(7)–2.039(7)	1.924–2.026
M–N_β	2.437(1)	2.576(13)	1.996(7)–2.100(7)	1.981–2.139
M–Cl	—	—	2.245(2)–2.622(2)	—
$(M\text{-}O_2N)_{min}$	2.637(1)	2.370(11)	2.836(8)	2.745
M-OH_2	2.371, 2.386	2.375, 2.387	—	—
M···M[b]	4.089(1)	3.505(1)	3.104(2)	3.467
C-NO_2	1.447(2)	1.447(4)	1.434(12), 1.457(11)	1.447, 1.448
N–O	1.215(1), 1.233(2)	1.221(8), 1.231(7)	1.205(10)–1.224(10)	1.216–1.227
C–N_α	1.321(2), 1.322(1)	1.322(3), 1.338(3)	1.289(11)–1.340(12)	1.320–1.333
N_α–N_β	1.339(2), 1.342(1)	1.340(10), 1.341(14)	1.337(10)–1.358(10)	1.331–1.355
N_β–N_β	1.323(2)	1.347(12)	1.339(10), 1.344(10)	1.317, 1.325

[a] Minimal and maximal distances unless stated otherwise. [b] Shortest distance. [c] Data taken from ref. 33. [d] Data taken from ref. 8.

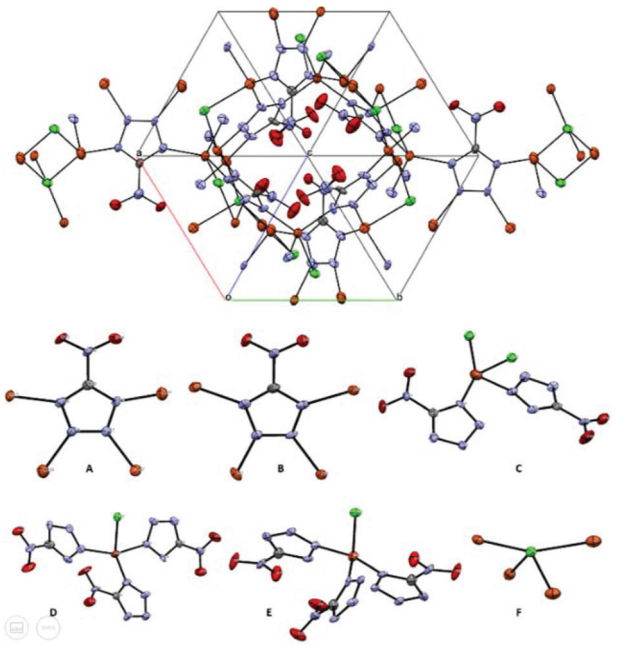

Fig. 3 Projections of the thermal ellipsoid in the molecular structure of the crystals of **3** (set at the 67% probability level) showing the unit cell (top, down 1, 1, –1 axis), the coordination of copper to the tetrazolato ligands (A and B), and the primary coordination sphere of copper (Cu (11), C; Cu(2), D; Cu(1), E), and chlorine (F); selected bond lengths Cu3–Cl1 2.371(2), Cu3–N7 2.027(8), Cu3–N6 2.065(7), Cu3–N9 2.039(7), Cu2–Cl1 2.561(3), Cu2–N4 2.028(7), Cu2–N2 2.067(7), Cu2–N5 1.996(7), Cu1–Cl1 2.245(2), Cu1–Cl1 2.622(3), Cu1–N3 2.100(7), Cu1–N1 1.968(7), Cl1–Cu3 2.371(2), Cl1–Cu2 2.561(3), Cl1–Cu1 2.622(3), O3–N10 1.205 (10), O4–N10 1.225(10), O2–N8 1.224(10), O1–N8 1.217(11), N10–C2 1.457(11), N4–N3 1.347(10), N4–C2 1.340(12), N3–Cu1 2.101(7), N3–N2 1.344(10), N2–Cu2 2.067(7), N2–N1 1.346(11), N1–C2 1.289(11), N7–N6 1.337(10), N7–C1 1.327(12), N6–Cu3 2.065(7), N6–N5 1.339(10), N5–N9 1.358(10), N9–Cu3 2.039(7), N9–C1 1.330(12), N8–C1 1.434(12).

$\mu^4(N_\alpha,N_\alpha',N_\beta,N_\beta')$-NT bridges (Fig. 3, middle; **2**, one N engaged in $\mu^2(N_\beta,O)$-NT; **4**, three or four engaged in $\mu^3(N_\alpha,N_\alpha',N_\beta)$-NT and $\mu^4(N_\alpha,N_\alpha',N_\beta,N_\beta')$-NT). As in **4**, the coordinative Cu–N_α bonds are slightly shorter (1.968(7)–2.027(7) Å) than those involving N_β ring-atoms (1.996(7)–2.100(7) Å), yet both are on average slightly longer (1 to 2 pm) than those found in **4** (see Table 2). The shortest Cu···O contact in compound **3** (2.836 Å), however, is somewhat longer than that found in **4** (2.745 Å). Similar to the finding for structures of **1** and **2**, the different coordination environments have only negligible effects on the molecular structure of the N_4C-NO_2 ligand, as neither the presence of Cl^- (**3** *vs.* **4**) nor the replacement of $Na(H_2O)_4^+$ by Cu^+ (**2** *vs.* **3**) change its internal bond lengths and angles in any significant way. The X-ray powder diffractogram predicted from the single crystal data is consistent with all diffractograms obtained from direct measurement of the powdery material of several batches obtained in the synthesis of **3** (see Fig. 4 and S3, S4†). The crystallographically determined density of compound **3** is significantly higher than that of **4** (2.939 g cm^{-3} *vs.* 2.584 g cm^{-3}) and also slightly greater than what can be predicted from **4** and CuCl (2.817 g cm^{-3}), and this suggests that

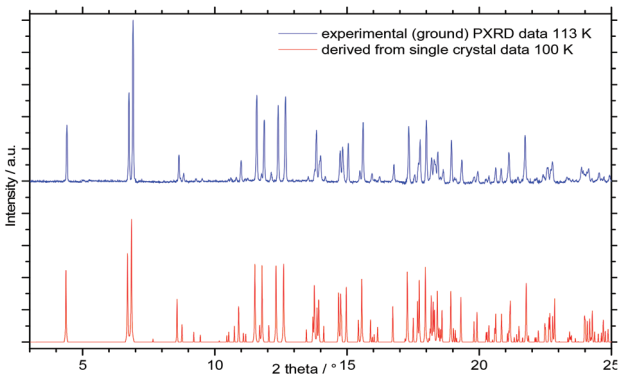

Fig. 4 Comparison of a simulated powder X-ray diffractogram of **3** based on the single crystal structure solution (–) with that obtained from measurement (–).

the packing in **3** is more efficient than in a simple mixed crystal with the 2 : 1 stoichiometry of Cu(N_4C-NO_2) and CuCl.

A similar argument can be made using the spatial demand of the CuN_4CNO_2 moiety: based on the effective volume of Cu(N_4C-NO_2) in **4** (114.1 Å^3), the volume available for Cu and Cl in **3** would only be 28.4 Å^3, which is much less than what is available in CuCl crystals (39.8 Å^3).

3.4 Spectral analysis

The transmission IR spectra of **3** and **4** are closely related (see Fig. S11 and S13†). Nevertheless, the region 1225 cm^{-1} to 1025 cm^{-1} is diagnostic and particularly suitable for a reliable identification and quantification of components (**3** and **4**) in mixtures of the two compounds (see Fig. 5). Both compounds can be mixed and milled in air (1600 min^{-1} rotary motion for 135 min using a 15 mm × 3 mm magnetic steel rod and a flat-bottomed PE vessel of 20 mm diameter) without initiation. The transmission IR spectra of the milled powders are linear combinations of the spectra of genuine **3** and **4** (see Fig. S19,† section shown in Fig. 5, bottom) and this shows that milling under these conditions occurs without the formation of another $Cu_xCl_y(N_4C$-$NO_2)_z$ phase, nor is the substance shown in Fig. 2 (middle) a new phase.

3.5 Thermal analysis

None of the investigated batches of **3** show thermal effects at temperatures between r.t. and the onset of decomposition. Therefore, the decomposing phase is the same as that present at r.t. The dynamics of the decomposition is dependent on the heating rate: at 10 K min^{-1}, decomposition is accompanied by extremely rapid heat release that causes the rupture of the sample confinement. At a rate of 3 K min^{-1}, however, a comparably slow decomposition takes place and this allows for a reliable integration of calorimetric curves in the range of the exothermic effect (see Fig. 6). Under identical conditions, the onset of decomposition of **3** occurs at a temperature (274 °C, T_{peak} = 283 °C, Fig. 6 top left), which in comparison is ~20 K below that of **4** (293 °C, T_{peak} = 305 °C, Fig. 6 top left).

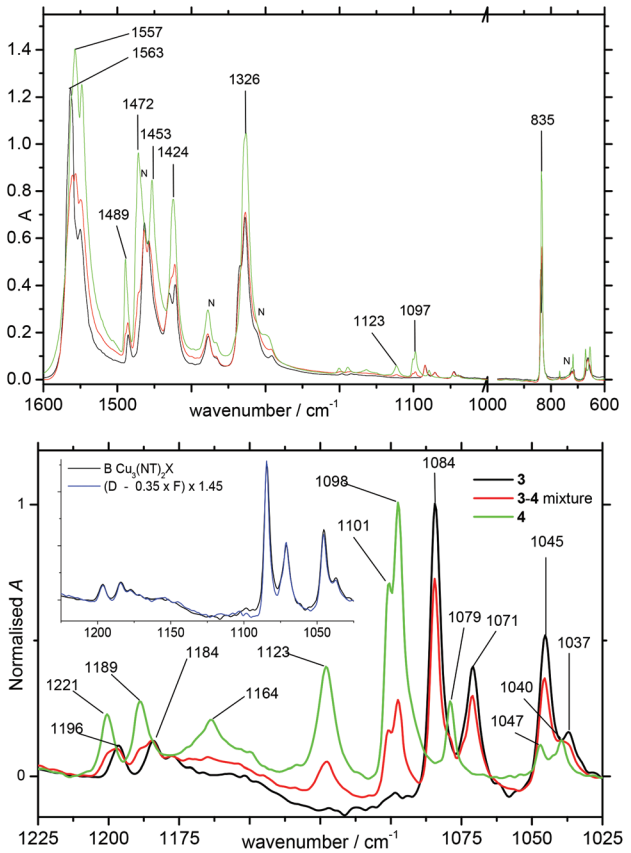

Fig. 5 Series of IR spectra. Top: Genuine **3** (—) and **4** (–) and a **3**–**4** mixture (–) all obtained directly from synthesis, in the range 1600–600 cm^{-1}; "N" denotes peaks mulling agent peaks. Middle: Layer of baseline-corrected, normalised spectra in the range 1225–1025 cm^{-1} to show that the **3**–**4** spectrum (–) is a linear combination of spectra of **3** (—) and **4** (–); see inset as proof, experimental (—) *vs.* {(**3**) − 0.35 × (**4**)} (–).

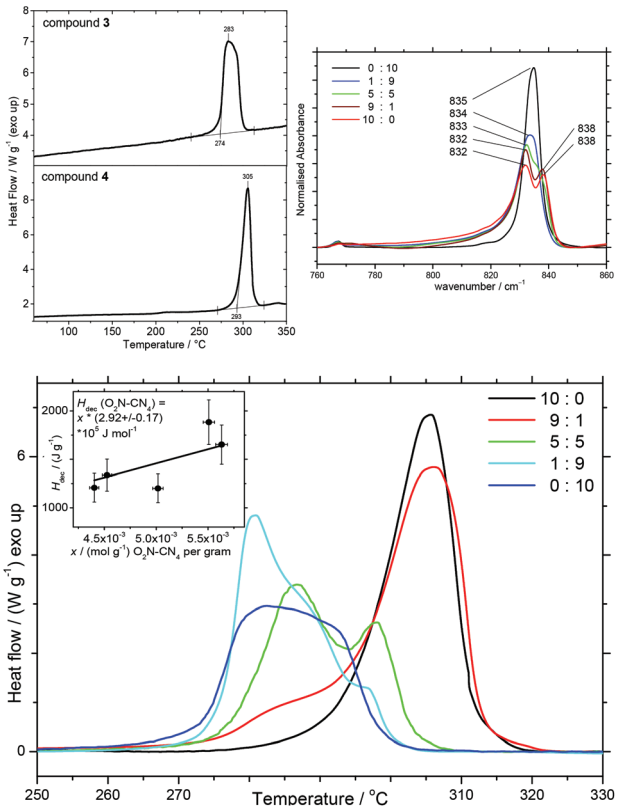

Fig. 6 DSC curves of **3** and **4** (top left) recorded in the temperature range 60 to 350 °C, and calorigrams of milled **3**–**4** mixtures (–, –, –) made from genuine **3** (–) and **4** (—) in the temperature range of decomposition (bottom), a scan rate of 3 K min^{-1} applies throughout; see Fig. 5 (bottom) for IR spectra correspondent to the mixtures. Diagnostic range in the IR spectrum of milled **3**–**4** mixtures featuring peaks at 832, 835 and 838 cm^{-1}, genuine **3** (–) and **4** (—) (top right).

Furthermore, compound **3** has a specific heat of decomposition (1201 J g^{-1}) that is 27% below that of **4** (1653 J g^{-1}), a molar heat of decomposition (based on Cu) that is only two thirds as large as that found for **4** (181.8 kJ mol^{-1} *vs.* 293.6 kJ mol^{-1}), and an energy density of the crystals that is 19% lower than **4** (3.5 kJ cm^{-3} *vs.* 4.3 kJ cm^{-3}). The ratio of molar heats of decomposition can thus be closely estimated by the ratio of stoichiometric proportions of copper and nitrotetrazolato groups in both compounds, (3 : 3)/(3 : 2) ≈ 0.67 (theory) *vs.* 0.62 (observed). Genuine samples of **3** and **4** have been mixed by co-grinding in ratios of 9 : 1, 5 : 5 and 1 : 9 (Fig. 6 bottom). Within the margins of errors, the enthalpies obtained thereof fit into the suggested dependency of mole fractions (inset Fig. 6, bottom), giving an effective molar enthalpy of decomposition per nitrotetrazolato group of 292(±17) kJ mol^{-1}. From the result obtained at a heating rate of 3 K min^{-1}, it can be concluded that the presence of chlorine has only a marginal influence on the distribution of the decomposition products originating from the nitrotetrazolyl group in the two compounds and their mixtures. Based on Kamlet and Jacobs' approach[38] to relating detonation pressure and detonation velocity to heats of detonation (as estimated by the heats of decomposition), detonation products and bulk densities, it becomes clear that **3** and **4** are closely related (41–42 *vs.* 34–36 kbar, 3.4–3.5 *vs.* 3.3–3.4 km s^{-1}), but inferior to lead azide (67 kbar, 3.8 km s^{-1})[39] on these performance criteria.

3.6 Stability and morphology

The stability of compound **3** was investigated toward air and water. According to results of IR spectroscopic and PXRD monitoring (Fig. S5†), compound **3** is stable indefinitely at r.t. in air. Complete decomposition, however, occurs within one month if samples are kept under deionized water exposed to air. The supernatant aqueous phase showed a pH of 6.10 (6.09 for compound **4**, 6.69 reported earlier), which did not change significantly over the course of several days. The decomposition is accompanied by the release of Cu^{2+} into the aqueous phase – a behaviour similar to the pH-dependent hydrolysis of copper(I) chloride in water,[40] which compound **4** is less likely to engage in due to the absence of Cl.

Untreated material of compound **3** that was obtained at a reduction temperature of 90 °C has a wider particle distribution (D_{10} = 31 μm; D_{50} = 71 μm, D_{90} = 149 μm) and a slightly

larger average particle size in comparison with material of compound **4** (23–34, 50–65, 86–120).

Intriguingly, microcrystals of compound **3** are significantly more impact sensitive than those of compound **4** (1.8(±0.2) J *vs.* 4.3(±0.3) J, see Fig. S20;† $Pb(N_3)_2$ for comparison 2.5–4.0 J;[14] Table S2† contains the summarised data). These differences are believed to originate in variations in crystal shape and the vibrational energy up-conversion efficiency[41] and this will be subject to a forthcoming paper.

3.7 Factors influencing the outcome of the reduction reaction

In our study consisting of a total of 21 consecutive trials, the influence of several synthetic parameters was investigated with an emphasis on the reproducibility of the synthesis of **3**. The comparably high yields of up to 86% thus far under optimal conditions allow for the tentative adoption of eqn (1).

$$3CuCl_2 + 2Na(N_4C-NO_2) + 1.5Na(HAsc) \rightarrow Cu_3Cl(N_4C-NO_2)_2 + 3.5NaCl + 1.5HCl + 1.5Asc \quad (1)$$

The outcome of the reduction reaction changed after several repetitions using the same apparatus. After five consecutive batches that produced compound **3**, another batch was obtained that consisted of a mixture of **3** and **4** (see Fig. 5, bottom, red spectral line); however, thereafter only compound **4** was obtained. The use of freshly crystallized $CuCl_2{\cdot}2H_2O$ instead of $CuCl_2$, distilled instead of deionized water, the halving of the reductant solution concentration, or a change of the reaction temperature within the range 80 to 95 °C had no significant effect on the course of the reduction. In order to obtain **3** again, the reaction vessel had to be cleaned by the action of hot concentrated nitric acid, and catalytic amounts of **3** obtained earlier needed to be added to the reaction mixture. We interpret this effect in terms of the action of a comparably small number of seed crystals. The application of **3** as seed increases the amount of **3** being produced. However, seed crystals of **4** outperform those of **3** by far. Intriguingly, the substitution of one-third (mol fraction) of $CuCl_2$ by $ZnBr_2$ or $NiCl_2$ under otherwise identical conditions also leads to the formation of compound **3**. Based on these observations, the following conclusions (i to vii) can be drawn: application of crystallised **1** without further purification as the nitrotetrazolate transfer reagent leads to the formation of powders that are neither **3** nor **4** (i) – an outcome attributed previously to the presence of trace-impurities that act in a catalytic mechanism inhibitive of the formation of either **3** or **4**. Within the conditions investigated by us, formation of either **3** or **4** requires the use of purified NaNT in the form of compound **2** (ii). The use of freshly crystallized $CuCl_2{\cdot}2H_2O$ instead of $CuCl_2$, or distilled instead of deionized water, or changing the concentration of the reductant solution, or changing the Cu^{2+}/N_4C-NO_2 ratio has, within certain limits, no significant effect on the course of the reduction (iii). The formation of the desired product requires the presence of the appropriate seed crystals, which induce the crystallisation of **3** and **4**, respectively (iv). The formation of **3** requires the absence of seed crystals of **4** (v). The seed crystals can be removed effectively by aqueous nitric acid (vi). A partial replacement of $CuCl_2$ by other metal chlorides ($ZnCl_2$) leads to the formation of **3** (vii). A summary of the factors can be found in Table S3.†

4. Conclusions

In the competitive reduction reactions of copper(II) chloride, a wine-red chlorine-containing copper nitrotetrazolate, $Cu_3Cl(N_4C-NO_2)_2$, was discovered. This result indicates that such reduction reactions produce a number of well-defined energetic materials. The formation of $Cu_3Cl(N_4C-NO_2)_2$ shows that mixed-ligand coordination frameworks are possible and lends weight to the notion that more efficient lead-free primary initiators are potentially accessible in which Cl is replaced by a different, potentially explosophoric group with the aim to reduce sensitivity toward water, and to tune sensitivity toward shock, friction and temperature. The selectivity of the $CuCl_2$ – sodium ascorbate – explosophoric group-transfer reduction reaction can be controlled by the action of seed crystals and this can be exploited to direct the reaction pathway. Even though stable in air indefinitely, $Cu_3Cl(N_4C-NO_2)_2$ decomposes under water within weeks. The crystals of $Cu_3Cl(N_4C-NO_2)_2$ consist of an elaborate void-less coordination network with a density exceeding that of DBX-1. It is more friction and impact sensitive than either DBX-1 ($Cu(N_4C-NO_2)$) or lead azide and decomposes violently upon rapid heating or shock. $Cu_3Cl(N_4C-NO_2)_2$ is a powerful explosive with energetic parameters similar to those of $Cu(N_4C-NO_2)$. A new form of the nitrotetrazolato anion transfer agent NaNT was introduced as the crystalline tetrahydrate $NaNT{\cdot}4H_2O$. $NaNT{\cdot}4H_2O$ can be regarded as an attractive alternative to the existing dihydrate because of its high purity and lower energy density.

Conflicts of interest

There are no conflicts to declare.

Acknowledgements

The authors thank the University of Sheffield for a studentship to BW and L. Brammer and T. Roseveare for assistance with some of the PXRD measurements, and Jon Veal with the particle sizer. This study was part-funded by the WSTC, UK, under grant no. 1059. Dedicated to Prof. Alan Welch on the occasion of his retirement from Heriot-Watt University.

Notes and references

1 (*a*) J. P. Agrawal, *High Energy Materials*, Wiley-VCH, 2010, p. 131ff; (*b*) T. M. Klapötke and N. Mehta, Lead–free Primary Explosives, *Propellants, Explos., Pyrotech.*, 2014, **39**, 7–8.

2 Y. Tang, C. He, D. A. Mitchell and J. M. Shreeve, Potassium 4,4′-Bis(dinitromethyl)-3,3′-azofurazanate: A Highly Energetic 3D Metal-Organic Framework as a Promising Primary Explosive, *Angew. Chem., Int. Ed.*, 2016, **55**, 5565–5567.

3 Q. Sun, Y. Liu, X. Li, M. Lu and Q. Lin, Alkali Metals–Based Energetic Coordination Polymers as Promising Primary Explosives: Crystal Structures, Energetic Properties, and Environmental Impact, *Chem. – Eur. J.*, 2018, **24**, 14213–14219.

4 D. Chen, H. Yang, Z. Yi, H. Xiong, S. Zhu and G. Zhu, C8N26H4: An Environmentally Friendly Primary Explosive with High Heat of Formation, *Angew. Chem., Int. Ed.*, 2018, **57**, 2081–2084.

5 Q. Sun, X. Li, Q. Lin and M. Lu, Dancing with 5-substituted monotetrazoles, oxygen-rich ions, and silver: towards primary explosives with positive oxygen balance and excellent energetic performance, *J. Mater. Chem. A*, 2019, **7**, 4611–4618.

6 H. Ji, L. Liu, Q. Sun, X. Li and M. Lu, First Structural Characterization of Solvate-Free Silver 5-Nitrotetrazolate and its Comparison with other Energetic Silver Compounds in Structure and Property, *Propellants, Explos., Pyrotech.*, 2019, **44**, 803–806.

7 (*a*) Q.-Y. Wang, L. Zhang, W.-M. He, L. Yang, C. Zhang, Z.-Y. Wang, R. Zhang, J.-H. Chen, S. Wang, S.-Q. Zang and T. C. W. Mak, High-performance primary explosives derived from copper thiolate cluster-assembled materials for micro-initiating device, *Chem. Eng. J.*, 2020, **389**, 124455; (*b*) T. M. Klapötke, C. M. Sabate and M. Rasp, Alkali and transition metal (Ag, Cu) salts of bridged 5-nitrotetrazole-derivatives for energetic applications, *Dalton Trans.*, 2009, 1825–1834.

8 J. W. Fronabarger, M. D. Williams, W. B. Sanborn, J. G. Bragg, D. A. Parrish and M. Bichay, DBX-1 – A Lead Free Replacement for Lead Azide, *Propellants, Explos., Pyrotech.*, 2011, **36**, 541–550.

9 T. M. Klapötke, D. G. Piercey, N. Mehta, K. D. Oyler, M. Jorgensen, S. Lenahan, J. S. Salan, J. W. Fronabarger and M. D. Williams, Preparation of High Purity Sodium 5-Nitrotetrazolate (NaNT): An Essential Precursor to the Environmentally Acceptable Primary Explosive, DBX-1, *Z. Anorg. Allg. Chem.*, 2013, **639**, 681–688.

10 D. D. Ford, S. Lenahan, M. Jorgensen, P. Dube, M. Delude, P. E. Concannon, S. R. Anderson, K. D. Oyler, H. Chen, N. Mehta and J. S. Salan, Development of a Lean Process to the Lead-free Primary Explosive DBX-1, *Org. Process Res. Dev.*, 2015, **19**, 673–680.

11 N. Mehta, K. Oyler, G. Cheng, A. Shah, J. Marin and K. Yee, Primary Explosives, *Z. Anorg. Allg. Chem.*, 2014, **640**, 1309–1313.

12 T. M. Klapötke, D. G. Piercey, N. Mehta, K. D. Oyler and J. J. Sabatini, Reaction of Copper(I) Nitrotetrazolate (DBX-1) with Sodium m-Periodate, *Z. Naturforsch., B: J. Chem. Sci.*, 2014, **69**, 125–127.

13 E. v. Herz, Verfahren zur Herstellung von Nitrotetrazol, Patentschrift, DE1931H127723D 19310711 Nr 562511, 1931.

14 T. M. Klapoetke and C. M. Sabate, Safe 5-nitrotetrazolate anion transfer reagents, *Dalton Trans.*, 2009, 1835–1841.

15 M. H. V. Huynh, M. A. Hiskey, T. J. Meyer and M. Wetzler, Green primaries: environmentally friendly energetic complexes, *Proc. Natl. Acad. Sci. U. S. A.*, 2006, **103**, 5409–5412.

16 Y. Pu, D. Sheng, Y. Zhu, L. Chen, B. Yang, Y. Wang and M. Xu, Synthesis and characterization of copper(I) nitrotetrazolato, *Huogongpin*, 2009, 43–45.

17 Y.-L. Pu, D.-L. Sheng, Y.-H. Zhu, L.-K. Chen, B. Yang, Y.-L. Wang and M.-H. Xu, *Hanneng Cailiao*, 2010, **18**, 654–659.

18 T. Klapoetke and C. M. Sabaté, Less sensitive transition metal salts of the 5-nitrotetrazolate anion, *Cent. Eur. J. Energ. Mater.*, 2010, **7**, 161–173.

19 M. Krawiec, S. R. Anderson, P. Dube, D. D. Ford, J. S. Sala, S. Lenahan, N. Mehta and C. R. Hamilton, Hydronium Copper(II)-tris(5-nitrotetrazolate) Trihydrate - A Primary Explosive, *Propellants, Explos., Pyrotech.*, 2015, **40**, 457–459.

20 J. W. Fronabarger, M. D. Williams and S. Hartman, Copper (I) 5-nitrotetrazole Synthesis Optimization, NSWC-IH Contract 2010. May 25, VSE Corporation Customer, Pacific Scientific EMC, Chandler AZ, USA, PO F060467.

21 J. W. Fronabarger, M. D. Williams and W. B. Sanborn, Copper(I) 5-nitrotetrazolate synthesis as lead-free primary explosive, PCT Int. Appl., WO 2008048351 A2 20080424, 2008.

22 J. G. Bragg, J. B. Pattison, J. W. Fronabarger and M. D. Williams, Facile method for preparation of sodium 5-nitrotetrazolate using a flow system, PCT Int. Appl., WO 2016115564 A1 20160721, 2016.

23 J. W. Fronabarger, J. B. Pattison and L. F. W. Walsh, Purification of flow sodium 5-nitrotetrazolate solutions with copper modified cation exchange resin, U.S. Pat. Appl. Publ., US 20180111909 A1 20180426, 2018.

24 T. M. Klapoetke, D. G. Piercey, J. W. Fronabarger and M. D. Williams, Preparation of a lead-free primary explosive copper(I) 5-nitrotetrazolate, U.S. Pat. Appl. Publ., US 20150239910 A1 20150827, 2015.

25 J. W. Fronabarger and M. D. Williams, Preparation of a lead-free primary explosive, PCT Int. Appl.,WO 2010085583 A1 20100729, 2010.

26 S. R. Qiu, B. C. Wood, P. R. Ehrmann, S. G. Demos, P. E. Miller, K. I. Schaffers, T. I. Suratwala and R. K. Brow, Origins of optical absorption characteristics of Cu^{2+} complexes in aqueous solutions, *Phys. Chem. Chem. Phys.*, 2015, **17**, 18913–18923.

27 G. M. Sheldrick, *SADABS, Empirical absorption correction program based on the method of Blessing*.

28 L. Krause, R. Herbst-Irmer, G. M. Sheldrick and D. Stalke, An empirical correction for absorption anisotropy, *J. Appl. Crystallogr.*, 2015, **48**, 3–10.

29 R. H. Blessing, An Empirical Correction for Absorption Anisotropy, *Acta Crystallogr., Sect. A: Found. Crystallogr.*, 1995, **51**, 33–38.

30 Bruker, *SADABS*, Bruker Axs Inc., Madison, Wisconsin, USA, 2016.

31 O. V. Dolomanov, L. J. Bourhis, R. J. Gildea, J. A. K. Howard and H. Puschmann, H. OLEX2: a complete structure solution, refinement and analysis program, *J. Appl. Crystallogr.*, 2009, **42**, 339–341.
32 G. M. Sheldrick, Crystal structure refinement with SHELXL, *Acta Crystallogr., Sect. C: Struct. Chem.*, 2015, **71**, 3–8.
33 T. M. Klapoetke, C. M. Sabate and J. M. Welch, Alkali metal 5-nitrotetrazolate salts: prospective replacements for service lead(II) azide in explosive initiators, *Dalton Trans.*, 2008, 6372–6380.
34 T. M. Klapoetke, C. M. Sabate and J. M. Welch, Preparation and crystal structures of two salts with the 5-nitrotetrazolate anion, *Heteroat. Chem.*, 2009, **20**, 35–44.
35 G. A. Bain and J. F. Berry, Diamagnetic Corrections and Pascal's Constants, *J. Chem. Educ.*, 2008, **85**, 532–536.
36 J. M. Knaust and S. W. Keller, A mixed-ligand coordination polymer from the in situ, Cu(I)-mediated isomerization of bis(4-pyridyl)ethylene, *Inorg. Chem.*, 2002, **41**, 5650–5652.
37 M. Du, C.-P. Li, C.-S. Liu and S.-M. Fang, Design and construction of coordination polymers with mixed-ligand synthetic strategy, *Coord. Chem. Rev.*, 2013, **257**, 1282–1305.
38 M. J. Kamlet and S. J. Jacobs, Chemistry of Detonations, I. A Simple Method for Calculating Detonation Properties of C–H–N–O Explosives, *J. Chem. Phys.*, 1968, **48**, 23–35.
39 R. Matias and J. Pachmann, *Primary Explosives*, Springer Heidelberg, New York, Dordrecht, London, 2013, p. 79ff.
40 H. Liu, Y. Zhou, S. A. Kulinich, J.-J. Li, L.-L. Han, S.-Z. Qiao and X.-W. Du, Second law analysis of CuCl2 hydrolysis reaction in the Cu-Cl thermochemical cycle of hydrogen production, *J. Mater. Chem. A*, 2013, **1**, 302–307 and literature cited therein.
41 A. A. L. Michalchuk, M. Trestman, S. Rudić, P. Portius, P. T. Fincham, C. R. Pulham and C. A. Morrison, *J. Mater. Chem. A*, 2019, **7**, 19539–19553; and literature cited therein.